Compact RF non-linear electro thermal model of SiGe HBT for the design of broadband ADC's

A. Saleh, A. El Rafei, M. Dieng, T. Reveyrand, R. Sommet, J.-M. Nébus and R. Quéré

Published in
International Journal of Microwave and Wireless Technologies, volume 4, issue 06, December 2012, pp. 569-578.

Crossref DOI: 10.1017/S1759078712000566

International Journal of Microwave and Wireless Technologies, 2012, 4(6), 569–578.
doi:10.1017/S1759078712000566

RESEARCH PAPER

Compact RF non-linear electro thermal model of SiGe HBT for the design of broadband ADC's

ALAA SALEH, ABDEL KADER EL RAFEI, MOUNTAKHA DIENG, TIBAULT REVEYRAND, RAPHAEL SOMMET, JEAN-MICHEL NEBUS AND RAYMOND QUERE

The design of high speed integrated circuits heavily relies on circuit simulation and requires compact transistor models. This paper presents a non-linear electro-thermal model of SiGe heterojunction-bipolar transistor (HBT). The non-linear model presented in this paper uses a hybrid π topology and it is extracted using IV and S-parameter measurements. The thermal sub-circuit is extracted using low-frequency S-parameter measurements. The model extraction procedure is described in detail. It is applied here to the modeling of npn SiGe HBTs. The proposed non-linear electro-thermal model is expected to be used for the design of high-speed electronic functions such as broadband analog digital converters in which both electrical and thermal aspects are engaged. The main focus and contribution of this paper stands in the fact that the proposed non-linear model covers wideband-frequency range (up to 65 GHz).

Keywords: Modelling, Simulation and Characterizations of devices and Circuits, Microwave Measurements

Received 10 March 2012; Revised 25 July 2012; first published online 29 August 2012

I. INTRODUCTION

Owing to superior speed performance, heterojunction-bipolar transistors (HBT) have found wide applications in high-speed switching and digital electronic systems. The demand for wideband circuits is driven by many newly introduced or future military and commercial applications, such as short-range high data rate communication systems, radar detection, digital satellite payloads and software-defined radios. Advances in modern processes such as SiGe heterojunction transistors have shown the possible practical realization of low-cost communication systems-on-chip (SOC). Owing to its high-speed advantage and great design flexibility, SiGe HBT has emerged as a technology of choice for radio-frequency (RF) and mixed digital/analog circuits [1]. Integrated circuit designers are often faced with model complexity versus simulation efficiency. It is highly desirable to have two kinds of models, a simplified version for fast simulations and circuit design tasks and a detailed version for process technology evaluation and device structure optimization. The contribution proposed in this paper concerns a compact non-linear electro-thermal model for circuit design purpose.

Most of the reported HBT models such as VBIC, MEXTRAM, and HICUM are very complex and have a great number of parameters [2–5]. In this paper, we propose a compact model that does not target a description of numerous physical phenomena that take place in the device. The aim of the proposed model is to provide a sufficiently accurate prediction of the main electro-thermal aspects to enable fast and efficient simulations for circuit design purpose. A hybrid model already reported in [6, 7] has been enhanced as shown in the following and is applied here to the non-linear electro-thermal modeling of SiGe HBT's from Infineon Technologies. The technology is called B7HF200 and uses relaxed 0.35 μm lithography. The process provides high-speed HBTs ($fT = 200$ GHz; $F_{max} = 250$ GHz) [8]. In Section II, the model topology is given; in Section III, the model extraction procedure is described; and Section IV is dedicated to model validation over a broadband.

XLIM – CNRS 123, Avenue Albert Thomas, 87060 Limoges Cedex, France
Corresponding author:
Alaa Saleh
Email: salehalaa83@gmail.com

II. NON-LINEAR MODEL TOPOLOGY

The electro-thermal HBT model used in this work is based on a hybrid π topology as illustrated in Fig. 1.

The intrinsic part of the equivalent circuit is described by four diodes and one controlled current source:

- *Dbe* and *Dbc* control the current source.
- *Dfbe* and *Dfbc* take into account leakage currents.

This model uses a physical description for base collector and base emitter charges.

Equations of such a model have been already reported and applied to GaAs HBT modeling in [6, 7]. They are recalled hereafter for convenience.

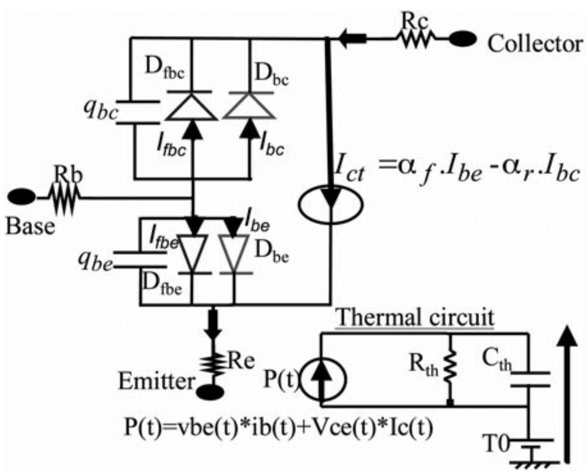

Fig. 1. Model topology.

The model parameters that are given below correspond to a $3 \times 2.8 \times 0.35\ \mu m^2$ SiGe HBT

1) Model equations for diodes:

$$I_{be} = I_{se}e^{-Te/T}(e^{qVbe/NekT} - 1) \tag{1}$$

$$I_{bc} = I_{sc}e^{-Tc/T}(e^{qVbc/NckT} - 1) \tag{2}$$

$$I_{fbe} = I_{sfe}e^{-Tfe/T}(e^{qVbe/NfekT} - 1) \tag{3}$$

$$I_{fbc} = I_{sfc}e^{-Tfc/T}(e^{qVbc/NfckT} - 1) \tag{4}$$

T is the junction temperature, k is the Boltzmann constant, and q is the electron charge.

Model parameters for diodes

$I_{Se} = 500$ A	$I_{Sc} = 20\ 000$ A	$I_{Sfe} = 0.005$ A	$I_{Sfc} = 1000$ A
$T_e = 12\ 498$ K	$T_c = 15\ 440$ K	$T_{fe} = 8000$ K	$T_{fc} = 14\ 500$ K
$Ne = 1.097$	$Nc = 1.004$	$Nfe = 2.1$	$Nfc = 3$

2) Model equations for current source I_{ct}

$$I_{ct} = \alpha_f I_{be} - \alpha_r I_{bc} \tag{5}$$

$$\alpha_f = \frac{\beta o}{\beta o + 1} \text{ and } \alpha r = \frac{\beta r}{\beta r + 1} \tag{6}$$

Model parameters for current source, access resistances, and thermal circuit

$\beta o = 343$	$\alpha r = 1$	$Rb = 10.04\ \Omega$	$Re = 2.98\ \Omega$
$Rc = 18.11\ \Omega$	$To = 273\ ^\circ K$	$R_{th} = 1600^\circ$ C/W	$C_{th} = 10^{-9}$ J/°C

3) Model equations for charges:

3a) Base-emitter charge q_{be}

$$q_{be} = q_{bej} + q_{bed} + q_{bek} \tag{7}$$

q_{bej} stands for depletion, q_{bed} for diffusion, and q_{bek} for Kirk effect.

$$q_{bej} = \frac{-C_{jeo}\varphi_{BE}\left(1 - (V_{lim-be}/\varphi_{BE})\right)^{1-Mje}}{1 - Mje} + \frac{C_{jeo}}{(1 - lim)^{Mje}}(Vbe - V_{lim-be}) + K_{be} \tag{8}$$

$$\text{With} \quad V_{lim-be} = Vbe - \phi_{BE}(1 - lim) \, Ln(1 + e^{(Vbe - lim\cdot\phi_{BE}/\phi_{BE}(1-lim))}) \tag{9}$$

K_{be} is a constant that is used to force the charge to 0 when $Vbe = 0$ V. V_{lim-be} expression is used to limit the value of the base emitter voltage Vbe when it approaches Φ_{BE}. This technique has been reported in [9].

Model parameters for q_{bej}

$C_{jeo} = 2.1 \times 10^{-14}$ F	$\phi_{BE} = 0.6$ V	$M_{je} = 0.008$	$K_{be} = 0.95$ C	$Lim = 0.98$

$$q_{bed} = \tau_{fo}(1 - V_{bci}V_{bc})(1 - I_{ci}Ic)(1 - F_{cd})F(Ic) \tag{10}$$

Ic is the collector current and $F(Ic)$ is a function defined as following:

$$F(Ic) = Ic + A_{\tau f}G\left(\frac{-Ic}{A_{\tau f}}\right) \quad \text{if} \quad Ic > 0$$

$$F(Ic) = A_{\tau f}G\left(\frac{Ic}{A_{\tau f}}\right) \quad \text{if} \quad Ic < 0$$

Where function $G(u) = \dfrac{0.5}{\sqrt{1 + u^2} - u}$ if $u > -1$

$$G(u) = \frac{-0.5}{u(1 + \sqrt{1 + (1/u^2)})} \quad \text{if} \quad u < -1$$

Model parameters for q_{bed}

$\tau_{fo} = 10^{-13}$ s	$V_{bci} = 1$	$I_{ci} = 5 \times 10^{-3}$	$F_{cd} = 0.259$	$A_{\tau f} = 0.01$

$$q_{bek} = \tau_{ko}Ic(1 - F_{ck})H^2(Ic) \tag{11}$$

Function $H(Ic)$ is defined as the following and has also been used in [10].

$$H(Ic) = \frac{(1 - (I_k/Ic + 10^{-6}) + \sqrt{(1 - (I_k/Ic + 10^{-6}))^2 + A_{\tau k}}}{1 + \sqrt{1 + A_{\tau k}}} \tag{12}$$

where $I_k = I_{ko}(1 - Vbc_{invk}Vbc)$

Model parameters for q_{bek}

$\tau_{ko} = 1.7 \times 10^{-13}$ s	$F_{ck} = 0.7$	$I_{ko} = 11 \times 10^{-3}$A	$A_{\tau k} = 0.046$	$Vbc_{invk} = 0.2$ V

3b) Base-collector charge q_{bc}

$$q_{bc} = q_{bcj} + q_{bcd} + q_{bc-trans} \tag{13}$$

$$q_{bcj} = \frac{-C_{jco}\phi_{BC}\left(1 - (V_{lim-bc}/\phi_{BC})\right)^{1-Mjc}}{1 - M_{jc}} + \frac{C_{jco}}{(1 - lim)^{Mjc}}(Vbc - V_{lim-bc}) + Cbcp.Vbc \tag{14}$$

$$\text{With} \quad V_{\lim-bc} = Vbc - \phi_{BC}(1 - \lim) \; Ln(1 + e^{(Vbc - \lim\phi_{BC}/\phi_{BC}(1-lim))}) \tag{15}$$

Model parameters for q_{bej}

$C_{jco} = 3.8 \times 10^{-14}$ F	$\phi_{BC} = 1.2$ V	$M_{jc} = 0.4$	$Cbcp = 2^{-15}$ F	$lim = 0.98$

$$q_{bcd} = \tau_r Ic \tag{16}$$

$$q_{bc-trans} = F_{cd}q_{bed} + \frac{F_{ck}}{1 - F_{ck}}q_{bek} \tag{17}$$

F_{cd}: is a constant used to divide the charges in the base into two parts. The first one takes into account the diffusion charges which depend on Vbe, the second one $q_{bc-trans}$ takes into account non-quasi-static effects in charge distribution and is called *trans*-capacitance.

F_{ck}: is a constant used to divide the Kirk charges into a base emitter capacitance and a base collector capacitance.

q_{bek}: represents the part of qbc charges that appear at high-current densities due to the Kirk effect.

Cbc_p: represents the package capacitance

Model parameters for q_{bed} and q_{bek}

$\tau_r = 10^{-13}$ s	$F_{cd} = 0.259$	$F_{ck} = 0.7$

The new aspects in the model that are highlighted below are:

- Current gain formulation that fit current gain decrease versus collector current.
- Breakdown formulation.
- Temperature dependence of leakage diodes.
- Formulation of base collector charges for an improved cut-off frequency modeling.

Furthermore, a thermal impedance extraction technique already reported in [11, 12] is used and combined with the features mentioned above.

These aspects are successively reported in the following.

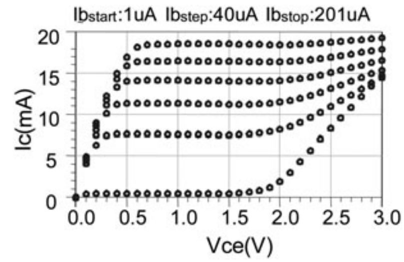

Fig. 2. DC IV measurements of a 3 × 2.8 × 0.35 μm² SiGe HBT.

III. MODELING ASPECT ENHANCEMENTS APPLIED TO NPN SIGE HBT

A) Current gain formulation

DC I/V characteristics of a 3 × 2.8 × 0.35 μm² SiGe HBT from Infineon Technologies have been measured using a Keithley 4200 semi-conductor device characterization system. During measurements the transistor is biased with a base current generator configuration [13]. The measurement results are given in Fig. 2.

Figure 3 shows the measured gain current characteristic of the transistor versus collector current.

It is observed that the current gain decreases versus collector current. In order to model this behavior, the following expression is used:

$$\beta = \beta_o + \beta_1 * \exp(-Ic/Ico), \tag{18}$$

where β_o, β_1 and Ico are the fitting parameters.

$\beta_o = 343$	$\beta_1 = 60$	$Ico = 7 \times 10^{-3}$ A

Figure 4(a) shows a comparison between simulated I/V plots and measurements when the model uses a constant gain ($\beta = \beta o$). Figure 4(b) shows the same comparison when the model uses a current gain that depends on the collector current.

It can be observed in Fig. 4(b) that the enhanced model provides a better fit of I/V characteristics at low current.

B) Breakdown model

For better convergence purpose, breakdown modeling is performed using equation (19)

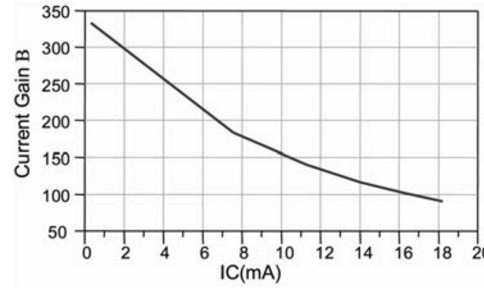

Fig. 3. Current gain versus collector current measured at $Vce = 1$ V.

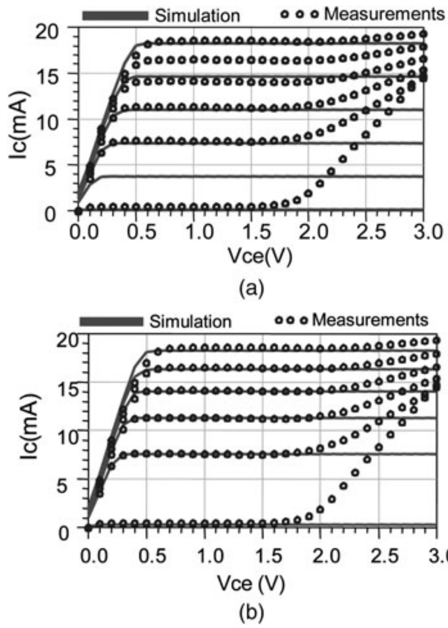

Fig. 4. Simulated IV network with constant current gain (a) and variable current gain versus collector current (b). (Ib_start 1 μA; Ib_step: 40 μA; and Ib_stop: 201 μA).

$$\alpha_f = \alpha_0(1 + \exp(Vce^2 - C - \lambda.IC)) \tag{19}$$

where C and λ are the fitting parameters. C parameter determines the breakdown voltage for a given collector current and λ takes into account the decrease of break down voltage at high collector currents. A good agreement between measurements and simulated results is illustrated in Fig. 5.

$\alpha_o = 0.975$	$C = 3.8$	$\lambda = 150$

C) Base collector charge formulation

The determination of cut-off frequencies and particularly the transition frequency is very important.

The transition frequency Ft is determined by computing the current gain from S-parameter measurements up to 65 GHz and by extrapolating the current gain at higher frequencies,

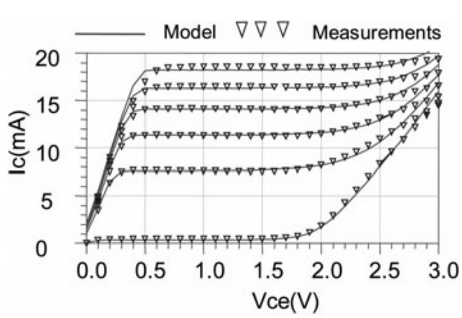

Fig. 5. Simulated and measured IV network with breakdown modeling. (Ib_start = 1 μA; Ib_step = 40 μA; and Ib_stop = 201 μA).

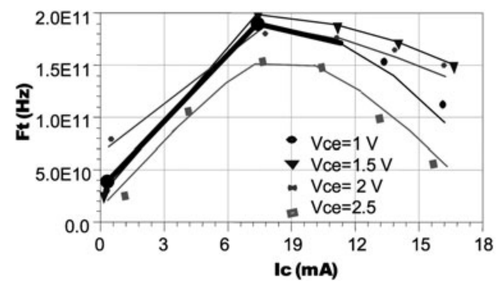

Fig. 6. Transition frequency versus collector current.

until it reaches 0 dB. Analytical expression of gain current h_{21} deduced from S parameters is given in equation (20).

$$h_{21} = \frac{2S_{12}}{(1 - S_{11})(1 + S_{22}) + S_{12}S_{21}} \tag{20}$$

In order to obtain correct behavior of the non-linear model at high-current densities and high collector emitter voltages, the base collector charges have been modeled by the following expressions:

$$\begin{aligned} qbc &= qbcj + qbc\_kirk + qbc\_Vcb \\ qbc\_kirk &= \tau_{ko}(1 + tanh(1 \times 10^{-3}(Ic - I_{ck})))(Ic^2) \end{aligned} \tag{21}$$

$$qbc\_Vcb = -Cbc\exp(Vcb - V_{cbo}) \tag{22}$$

$\tau_{ko} = 1.7^{-13}$ s	$I_{ck} = 11^{-3}$ A	$Cbc = 20$ fF	$V_{cbo} = 1.5$ V

The equations (21) and (22) replace equations (14), (16) and (17). The increase of base collector capacitance with respect to collector current enables the modeling of transition frequency saturation at high collector current (Kirk effect) as shown in Fig. 6.

The increase of base collector capacitance with respect to collector-base voltage also enables a good fit of transition frequency saturation at high collector base voltages as shown in Fig. 7.

D) Leakage diode temperature dependence

In order to characterize thermal dependence, Ic versus Vce DC measurements are performed at different chuck temperatures as shown in Fig. 8

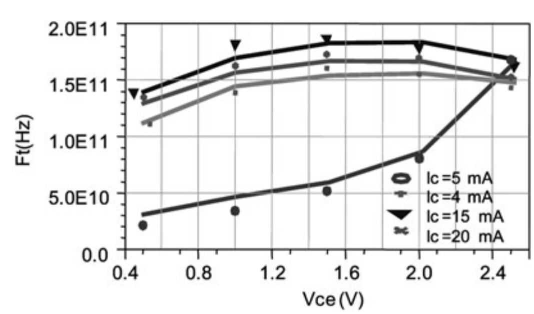

Fig. 7. Transition frequency versus collector emitter voltage.

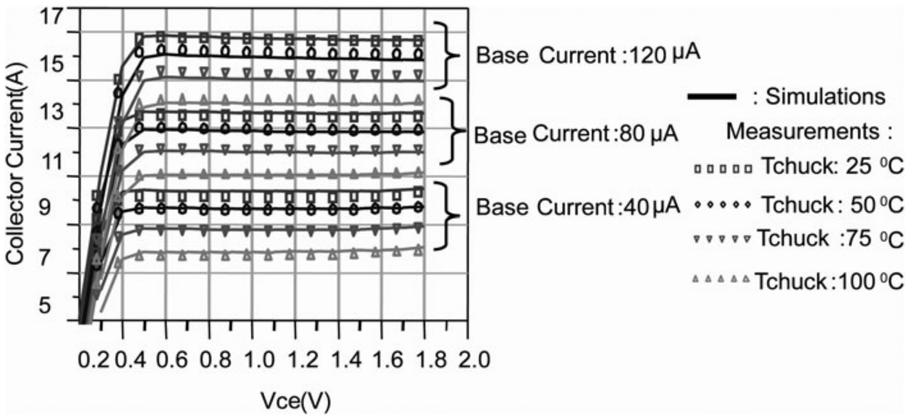

Fig. 8. Simulated and measured *Ic* versus *Vce* for different chuck temperature.

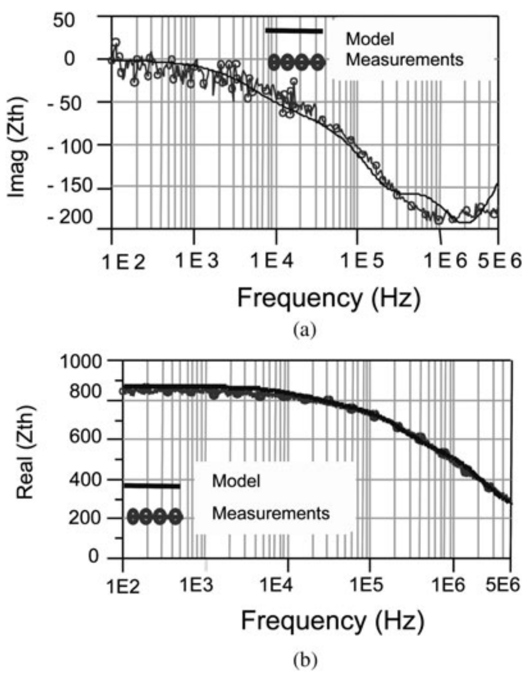

Fig. 9. (a) Imaginary part of thermal impedance. (b) Real part of thermal impedance.

Table 1. Scaling rules of model parameters X_u denotes the value of the parameter X for $A_E = 2.94\ \mu m^2$ (emitter area for the smallest transistor $3 \times 2.8 \times 0.35\ \mu m^2$).

Model parameter	Scaling law
Emitter resistance	$R_E = 2.98 - \left(\frac{0.4}{1.12}\right)(A_E - 2.94)$
Current gain	$\beta = \beta_o + B_1 Exp\left(-\frac{Ic}{Ico}\right)$
$\beta_o = \beta_o\_u + 18.4\left(1 - \exp\left(-\frac{(AE - 2.94)}{0.3}\right)\right)$	
$\beta_1 = \beta_1\_u + 50\left(1 - \exp - \left(\frac{(AE - 2.94)}{0.3}\right)\right)$	
$Ico = Ico\_u + 3.5e - 3\left(1 - \exp\left(-\frac{AE - 2.94}{0.3}\right)\right)$	
Collector resistance	$Rc = 30 - \left(\frac{18}{1.12}\right)(A_E - 2.94)$
Thermal resistance	$\mathrm{Rth} = \mathrm{Rth\_u} - \left(\frac{440}{1.12}\right)(A_E - 2.94)$ $R_{TH}\_u = 830$
Base collector junction capacitance	$Cbcjo = Cbcjo\_u + \frac{(1e - 14)}{1.12}(A_E - 2.94)$
Kirk current	$Iko = 11e - 3 + \frac{(2e - 3)}{1.12}(A_E - 2.94)$
Base emitter diode saturation current	$ISE = ISE\_u + \left(\frac{400}{1.12}\right)(A_E - 2.94)$ $I_{SE}\_u = 500$

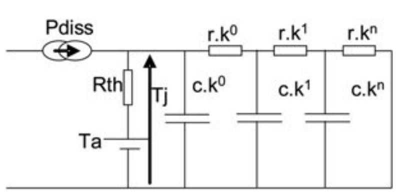

Fig. 10. Enhanced thermal sub circuit description.

It can be observed in Fig. 8 that the collector current decreases when the chuck temperature increases. However, for any fixed temperature and base current conditions, collector current does not decrease when collector voltage increases. Consequently, we have included in the model a temperature dependence of the current flowing in the base emitter leakage diode. The leakage current increases when the temperature increases. Leakage current variations versus

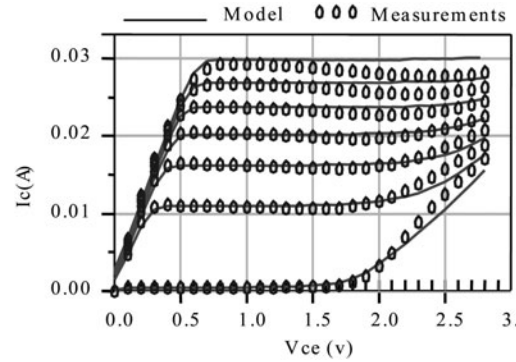

Fig. 11. Simulated and measured IV network (Ib_start = 1 μA; Ib_step = 50 μA; and Ib_stop = 301 μA).

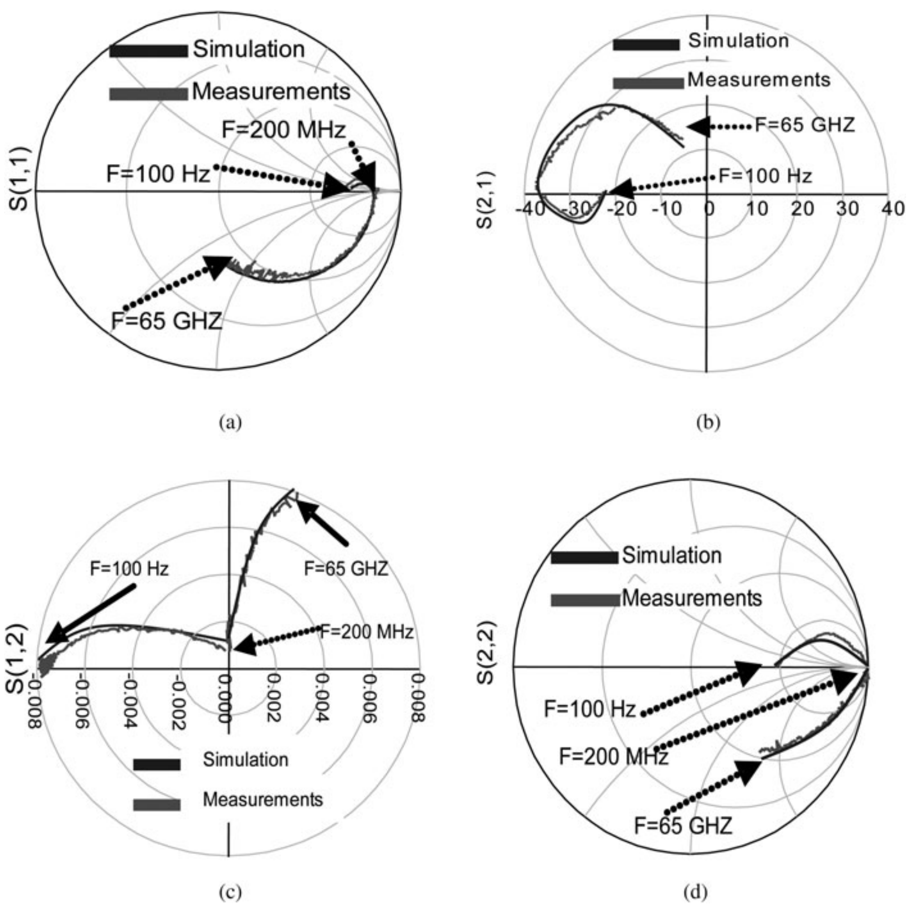

Fig. 12. (a) Measured versus simulated S11. (b) Measured versus simulated S21.(c) Measured versus simulated S12. (d) Measured versus simulated S22.

temperature are modeled by equation (23):

$$I_{sfe} = I_{sfeo} exp^{kT/qN_{FE}vt} \times exp^{-kT_{FE}/qN_{FE}vt}(exp^{Vbe/qN_{FE}vt} - 1) \tag{23}$$

where I_{sfeo}, T_{FE}, and N_{FE} are the fitting parameters.

$I_{sfeo} = 5 \times 10^{-3}$A	$T_{FE} = 8000$ K	$N_{FE} = 2.1$	$vt = 25$ mV

E) Thermal sub circuit determination

The thermal impedance profile versus frequency has been extracted using low-frequency *S* parameters method previously reported in [9]. The thermal impedance is extracted from the h_{12} parameter using the following relation:

$$Z_{th}(\omega) = \frac{h_{12}(\omega)}{\phi^* I_{Co}} \quad \text{where} \quad \phi = \frac{\partial Vbe}{\partial T} \tag{24}$$

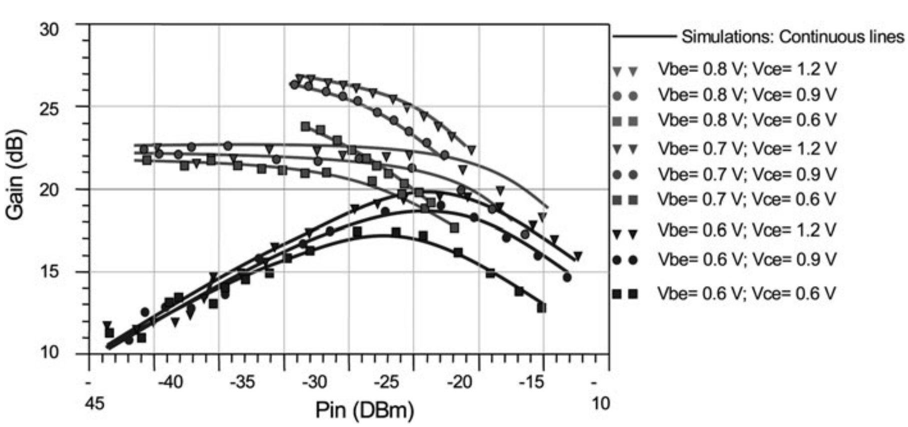

Fig. 13. Measured and simulated gain versus input power.

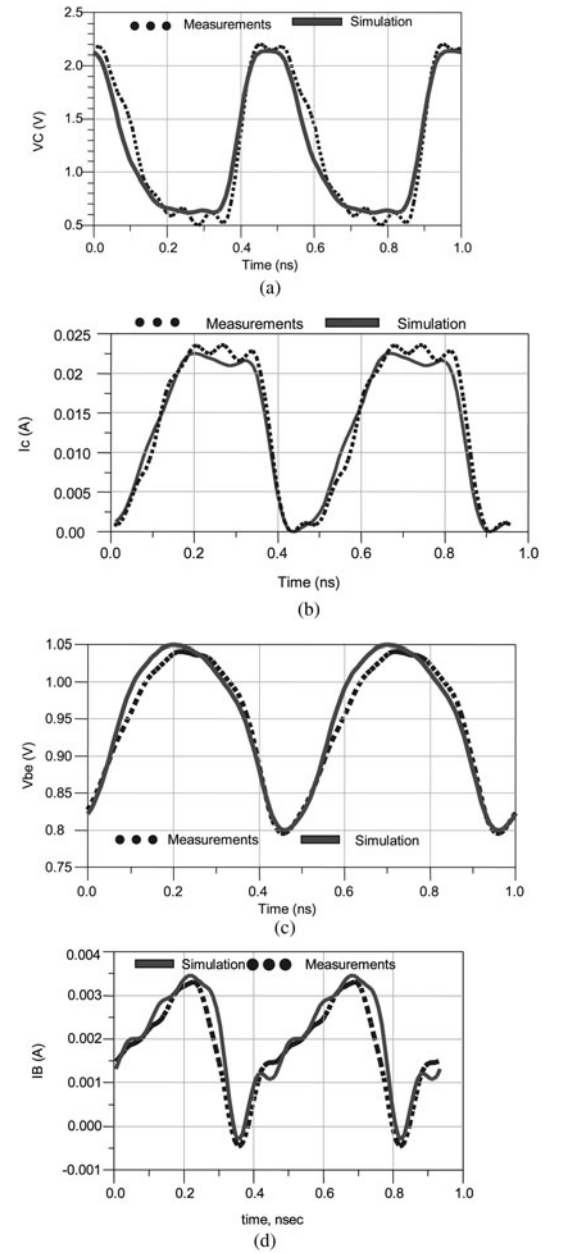

Fig. 14. Simulated and measured waveforms ($Vbe = 0.8$ V, $Vce = 1.2$ V, and input power $= -20$ dBm). (a) Collector emitter voltage. (b) Collector current. (c) Base emitter voltage. (d) Base current.

Following equation (24), it is clear that, for a given collector current I_{Co}, the only parameter to be determined is the base-emitter thermal coefficient ϕ. This coefficient is a technological parameter of the transistor that slightly depends on the collector current. It is taken here to be a value of -0.9 mV/°C.

Figures 9(a) and 9(b) show the real and imaginary parts of the thermal impedance measured in the (100 Hz–5 MHz) frequency range [14].

For a good description of thermal behavior, the thermal impedance symbolically represented in Fig. 1 by a single parallel RC network is substituted by a multi cell RC network as represented in Fig. 10 [12].

For a good agreement between measurements and simulations eight cells are considered. Model parameters are respectively:

$k = 2$	$R = 300$°C/W	$C = 10 \times 10^{-12}$ J/°C	$R_{TH} = 830$°C/W

k is a fitting parameter used to obtain a transient part of the thermal response close to a $\sqrt{T}$ shape (T is the temperature).

IV. MODEL SCALING

As the collector current flows through the emitter contact, ICo is proportional to the emitter area A_E. Thus, the proposed model can be scaled with respect to the emitter area. In this section, the scaling laws adopted for this model are given.

Table 1 gives a summary of the scaled parameters and their scaling rules. The model parameters are scaled with respect to the emitter area $A_{E.}$

Fig. 11 shows the simulated versus measured IV network for a $1 \times 10 \times 3.5$ μm^2.

V. MODEL VALIDATION

A) *S* parameters measurements

S parameters of the transistor are measured from 100 Hz to 65 GHz. The validation of the model over this frequency bandwidth is important for its use for the design of broadband analog digital converters.

Figure 12 shows a comparison between measured and simulated *S* parameters of a $3 \times 2.8 \times 0.35$ μm^2 SiGe HBT.

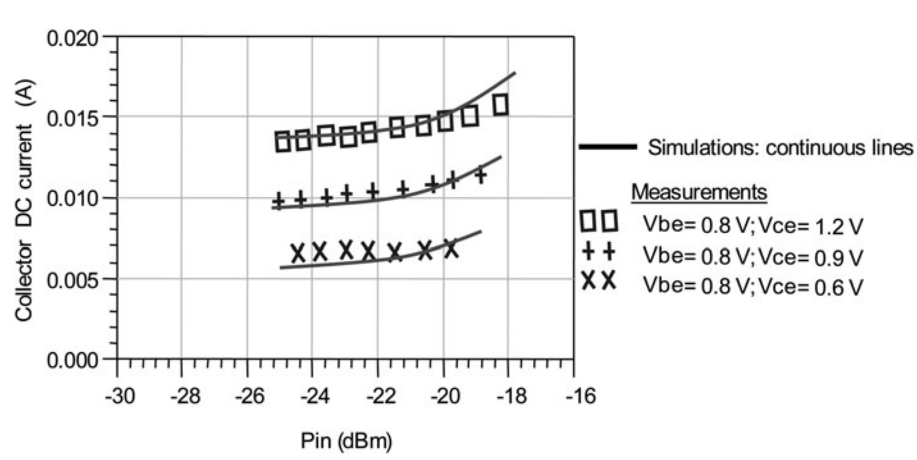

Fig. 15. Simulated and measured DC collector current.

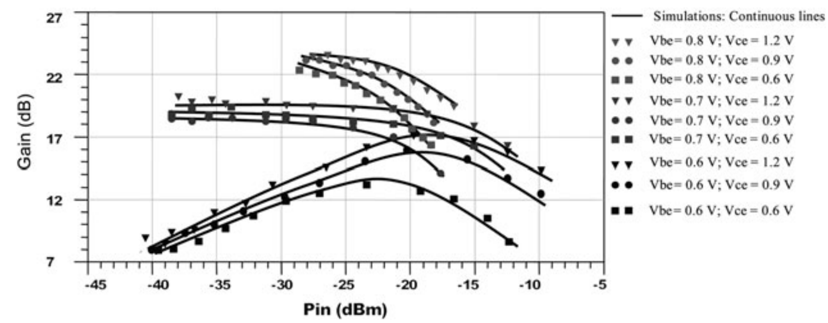

Fig. 16. Measured and simulated gain versus input power.

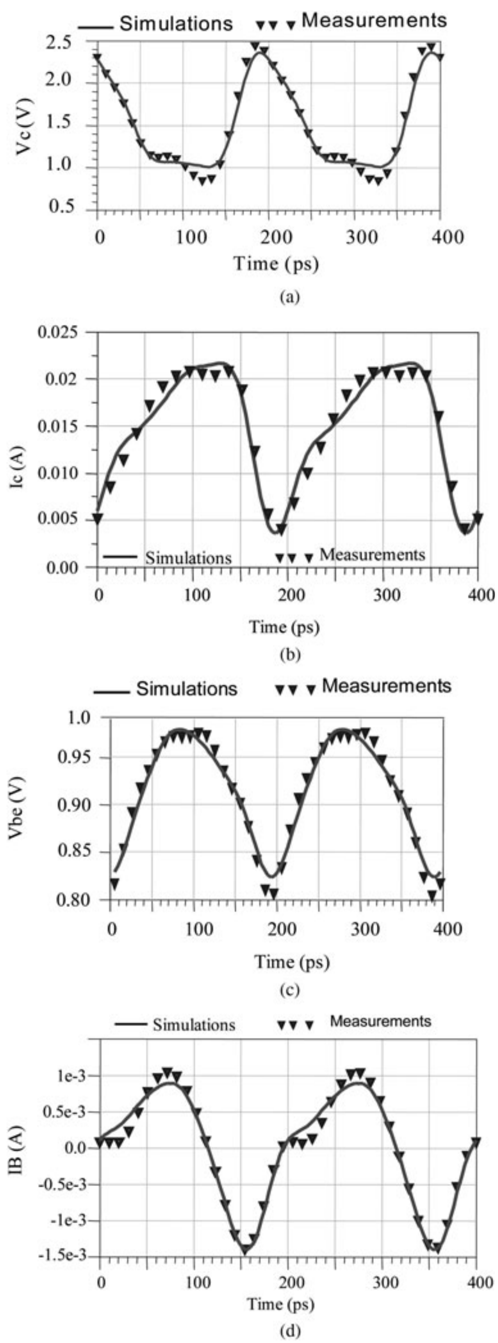

Fig. 17. Simulated and measured waveforms ($Vbe = 0.8$ V, $Vce = 1.2$ V, and input power $= -20$ dBm). (a) Collector emitter voltage. (b) Collector current. (c) Base emitter voltage. (d) Base current.

A good agreement between measured and simulated *S* parameters on the whole frequency bandwidth is obtained. It can be observed as two different regions in *S*-parameter loci. At low frequency, below 200 MHz, both thermal and electrical aspects are present and taken into account in transistor responses. For frequencies above 200 MHz, only electrical aspects impact transistor behavior.

B) Large signal measurements

Large signal measurements have consisted here in measuring the power gain of the transistor for different bias points and RF input power levels. CW measurements given below are performed at 2 GHz. The transistor under test is terminated into a 50 Ω load.

The power is swept from −40 to −12 dBm. Time domain current and voltage waveforms are obtained, thanks to the use of a vector network analyzer having time domain capabilities. We used for that purpose a large signal network analyzer (LSNA) with a calibrated phase reference generator [15].

Figures 13–15 show a comparison between simulated and measured power gain, voltage and current waveforms, and collector DC current.

Same measurements are performed at 5 GHz.

Figures 16–18 show a comparison between simulated and measured power gain, voltage and current waveforms, and collector DC current.

VI. CONCLUSION

In this paper, an accurate HBT Electro-Thermal compact model has been proposed. It has been shown that very small thermal time constants are involved in SiGe HBTs. Moreover, the non-linear model can easily be implemented in CAD software for the simulation of circuits such as power amplifiers or ADCs.

ACKNOWLEDGEMENTS

The authors acknowledge K. Aufinger from Infineon Technologies for providing the transistors. The research leading to these results has received funding from the European Community's Seventh Framework Program (FP7/2007–2013) under grant agreement no. 242521.

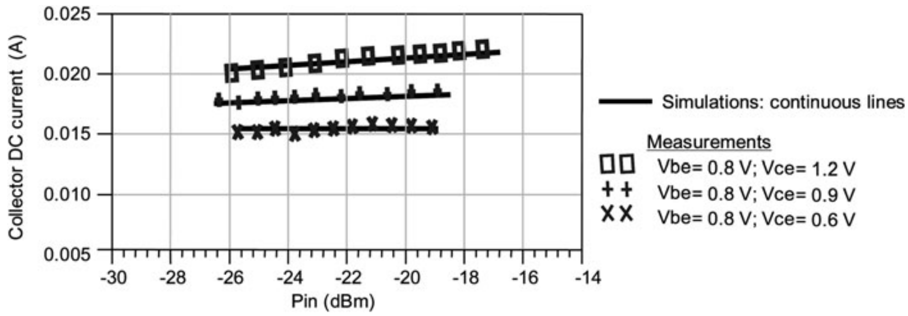

Fig. 18. Simulated and measured DC collector current.

REFERENCES

[1] Cressler, J.D.: Silicon–germanium as an enabling technology for extreme environment electronics. IEEE Trans. Devices Mater. Reliab., **10** (2010), 437–448.

[2] De Graaff, H.C.: State of the art in compact modelling with emphasis on bipolar RF circuit design, In Delft University of Technology. Solid-State Device Research Conf., September 1997, 14–23.

[3] Bhattacharyya, A.; Fregonese, S.; Maneux, C.; Zimmer, T.: Modeling of SiGe spike mono emitter HBT with HICUM in static and dynamic operations, In IEEE Bipolar/BiCMOS Circuits and Technology Meeting (BCTM), 2011, 53–56.

[4] Schroter, M.: HICUM/Levelo - a simplified compact bipolar transistor model Bipolar/BiCMOS Circuits and Technology Meeting, 2002. Proceedings of the 2002, 112–115.

[5] Bo, Han.; Shoulin, Li.; Jiali, Cheng.; Qiuyan, Yin.; Jianjun, Gao.: MEXTRAM model based SiGe HBT large-signal modeling. Journal of Semiconductors 2010, **31** (31), 104004-1–104004-6.

[6] Xiong, A. et al.: An electrothermal model of high power HBTs for high efficiency L/S band amplifiers, In Microwave Integrated Circuit Conf., 2008, 318–321.

[7] Jardel, O. et al.: An electrothermal model for GaInP/GaAs power HBTs with enhanced convergence capabilities, In European Microwave Integrated Circuits Conf., 2006, 296–299.

[8] Decoutere, S. et al.: Advanced process modules and architectures for half-terahertz SiGe:C HBTs, In Bipolar/BiCMOS Circuits and Technology Meeting (BCTM), 2009, 9–16.

[9] Paasschens, J.C.J.; Toorn, R.V.D.; Kloosterman, W.: The Mextram Bipolar Transistor Model level 504.6. Koninklijke Philips Electronics NV 2000/2005, March 2005.

[10] Schroeter, M.: RF–Modeling of Bipolar Transistors with HICUM, Chair for Electron Devices and Integrated Circuits, Lausanne University of Technology, Dresden, Germany, 2000.

[11] El Rafei, A.; Sommet, R.; Quere, R.: Electrical measurement of the thermal impedance of bipolar transistors. IEEE Electron Device Lett., **31** (9) (2010), 939–941.

[12] Sahoo, A.K.; Fregonese, S.; Zimmer, T.; Malbert, N.: Thermal impedance modelling of sige hbts from low frequency small signal measurements. IEEE Electron Device Lett., **32** (2011), 119–121.

[13] Saleh, A. et al.: 40 ns pulsed I/V setup and measurement method applied to InP HBT characterisation. Electron. Lett., **45** (2009), 286–287.

[14] El Rafei, A. et al.: DC (10 Hz) to RF (40 GHz) output conduction extraction by *S*-parameters measurements for in-depth characterization of AlInN/GaN HEMTS, focusing on low frequency dispersion effects, In EuMW2011, Manchester, October 2011, 5–8.

[15] Reveyrand, T.; Mallet, A.; Nebus, J.M.; Vanden Bossche, M.: Calibrated measurements of waveforms at internal nodes of MMICs with a LSNA and high impedance probes, In 62nd ARFTG Conf. Digest, December 2003, 71–76.

Alaa Saleh was born in Saida, Lebanon on August 1983. He received his Ph.D. from the XLIM laboratory in LImoges in 2009. His research interests include high-frequency transistor modeling for high-speed digital circuits applications as well as for microwave samplers.

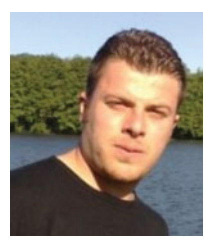

Abdelkader El Rafei was born in Akkar, Lebanon on May 29, 1985. He received a Ph.D. from the University of Limoges-XLIM laboratory in 2011. His research interests include high-frequency transistors, characterization, and conception of the dispersion effects including thermal and traps with low-frequency S-parameters measurement.

Mountakha Dieng was born in Kebemer, Senegal on June 10, 1982. He received a Ph.D. from the XLIM laboratory in Limoges. His research interests include evaluation of thermo-mechanical stress in plastic packaging for space environment.

Tibault Reveyrand (M'07) received a Ph.D. degree from the University of Limoges, France, in 2002. From 2002 to 2004, he was a Post-Doctoral Scientist with CNES (French Space Agency). In 2005, he worked as a CNRS engineer at XLIM (formerly IRCOM). His research interests include the characterization and modeling of radiofrequency (RF) and microwave non-linear components and devices. Dr Reveyrand was the recipient of the 2002 European GaAs best paper award.

Raphael Sommet received the French aggregation degree in applied physics and the Ph.D. degree from the University of Limoges, Limoges, France, in 1991 and 1996, respectively. Since 1997, he has been a permanent researcher at XLIM-CNRS at the University de Limoges. His research interests concern heterojunction-bipolar transistor (HBT) device simulation, 3D thermal finite-element simulation, model order reduction, microwave circuit simulation, and generally the coupling of all physics-based simulation with circuit simulation.

Jean Michel Nébus received a Ph.D. degree in electronics from the University of Limoges, France, in 1988. He has then worked for 2 years as a Project Engineer with Alcatel Space Industries, Toulouse, France. He is currently a Professor with the XLIM Laboratory, University of Limoges. His main research interests are non-linear microwave device characterization and power amplifier design.

Raymond Quere was born in 1954 in St Brieuc (France). He received an electrical engineering degree from ENSEEIHT Toulouse, France, in 1976 and the French aggregation in applied physics in 1978. After a teaching period of 8 years for undergraduate students, he prepared and earned a Ph.D. degree (with honors) from the University of Limoges in 1989. In 1992, he was appointed as a full time professor at the University of Limoges. From 1992 to 1997 he headed the Department of Electrical Engineering at the Institute of Technology of the University of Limoges. Since 1998, he has led the non-linear high-frequency devices, circuits and systems research department at XLIM-CNRS laboratory. He advises more than 30 Ph.D. students and he authors or coauthors more than 100 journal articles or communications in international conferences.